(4)

WSRL-TN-11/88

AR-005-395

THE RECONSTRUCTION OF AIRCRAFT TARGET TRAJECTORIES FROM HISTORICAL RADAR PLOT DATA

M.L. SCHOLZ

COMBAT SYSTEMS DIVISION
WEAPONS SYSTEMS RESEARCH LABORATORY

Approved for Public Release

AUGUST 1988

DSTO WSRL DEPARTMENT OF DEFENCE
DEFENCE SCIENCE AND TECHNOLOGY ORGANISATION

UNCLASSIFIED

TECHNICAL NOTE
WSRL-TN-11/88

THE RECONSTRUCTION OF AIRCRAFT TARGET TRAJECTORIES FROM HISTORICAL RADAR PLOT DATA

M.L. Scholz

A B S T R A C T (U)

An algorithm which can accurately reconstruct an aircraft target trajectory from pre-recorded digital radar plots is described. Periodically recorded track data from a tracking system provide the coarse target position and speed estimates required by the algorithm.

The algorithm has been applied in the operational analysis of the RAAF AN/TPS-43F(V)-1 surveillance radar and Myriad tracking systems at the No.2 Control and Reporting Unit (2CRU), Darwin, using data acquired during exercise Pitch Black 84-1. It has proven to be reliable and effective in localising targets in the presence of clutter and system noise. Several trajectories obtained using the algorithm are illustrated and compared with the corresponding track data.

Author's address:
Combat Systems Division
Weapons Systems Research Laboratory
PO Box 1700, Salisbury
South Australia

Requests to: Chief, Combat Systems Division

TABLE OF CONTENTS

LIST OF FIGURES

1. INTRODUCTION

The processing of targets by the AN/TPS-43F(V)-1 radar digital target extractor (DTE) was recently investigated from operational data recorded at the RAAF No 2 Control and Reporting Unit (2CRU) in Darwin during the air defence exercise Pitch Black 84-1(ref.1). An algorithm was employed during the analysis to discriminate DTE plots associated with aircraft targets from plots generated by clutter and internal system noise.

The algorithm has proven to be an effective and robust tool for accurately computing target trajectories from plot data in the presence of a high clutter and noise background. The technique, which essentially correlates plot centroids with periodically sampled target position and speed estimates from a tracking system, offers potential for the a-posteriori refinement of tracks in operational tracking systems.

2. PLOT EXTRACTION AND TARGET DISCRIMINATION

Multiple plots are extracted by the DTE from the radar video during each rotation, or scan, of the radar antenna. Each plot is a digital word of fixed length which contains information relevant to a single event. The three events which may cause a plot to be extracted include: the detection of a target in the radar or IFF video; the detection of radar jamming from the jam strobe video, or IFF jamming from the IFF video; and the traversal of the antenna through magnetic north (the "north-mark", or reference event) Due to the presence of bit flags and fixed data in certain fields, jam plots and real-time quality control (RTQC) plots, which respectively arise from jamming and north-mark events, are easily discernable from plots arising from target detections. Jam plots are therefore ignored in the following discussion, whilst the important role played by RTQC plots in the timing of analysis events is deferred for the present. Henceforth the unqualified term "plots" shall refer to the category of plots which are the result of target detections and RTQC plots shall always be explicitly labelled. Three types of plot are recognised according to the source of data (ie sensor): primary plots contain data only from the primary (ie radar) sensor; beacon plots contain data only from the beacon (ie IFF) receiver; and correlated plots contain data from both radar and IFF which pertain to the same (ie correlated) target.

The most important data in each plot are the range and azimuth of the two dimensional centre of mass, or centroid, of the target. The plot centroid is computed by the DTE from the pattern of signal returns in the radar or IFF video. Supplementary information in each plot may include IFF code data, target height measured by the radar, run length (azimuth extent of the target) and DTE internal status data, depending upon the type of plot.

Varying numbers of "false" plots (ie plots not associated with known targets) were observed in the output of the DTE during the exercise. Most were generated by the DTE from highly correlated clutter returns (for example, rain and terrain) and internal system noise where the correlation distances approximate the dimensions of the sliding window integrator used for target extraction.

A number of different methods for discriminating target-associated plots from false plots was initially investigated. Because the run length distribution of false plots significantly overlapped that of genuine plots (of the same type), a statistical discrimination method was not able to provide sufficient reliability. Exact methods were therefore examined. One such method relied upon detecting and classifying IFF code data and was thus restricted to beacon and correlated plots. Its usefulness was severely limited because many aircraft could not respond to IFF; they were either not equipped with IFF

transponders or, in the case of military aircraft, the transponders had been deliberately disabled. The majority of the plots recorded were found to be primary plots and so a method which relied instead upon classifying radar height data was examined. The usefulness of this method also proved to be limited because the radar height computer hardware responsible for supplying height validation strobes and height data to the DTE appeared to be malfunctioning during the exercise.

A method based upon matching plot centroids to known, approximate target positions was subsequently examined. Its main attraction is that it can function with all plot types. This method formed the basis of the algorithm which is described in detail in Section 3 (p 3). Although the reliability of the algorithm could not be mathematically established or validated because of the lack of suitable data, the algorithm appeared to work reliably in practice when applied to the recorded exercise data. With modification, the algorithm has the potential for application in operational tracking systems for the refinement of track positions and the management of crossing, splitting and merging tracks.

The coarse target position data required by the algorithm were obtained from track data recorded at the Myriad tracking system. Figure 1 (p 20) illustrates the data flow paths between the radar, DTE, Myriad tracking computer and the data recording system. Myriad was the only source of track data available during the exercise, but another (viz independent) source of data could have been utilised had it been available. There was a significant benefit in using Myriad data. Because the DTE supplied Myriad with plot data it was possible to measure the distribution of Myriad tracking errors with respect to the plot centroids. The algorithm provided the means of identifying the plots which corresponded to the selected targets. Although the tracking errors measured by this approach are not absolute (viz with respect to precise target positions), the additional errors introduced by the DTE in computing target centroids are negligible. Moreover, the tracking error of any target of opportunity can be determined and therefore a large sample of errors for statistical testing can be obtained. This method obviates the need for equipping targets with very sophisticated global position monitoring equipment, which is only warranted at the limits of the detection range where azimuthal errors in the computation of the target centroid become significant.

The algorithm in fact contains two distinct and independent procedures, referred to as Phases I and II. In Phase I, plots are selected for further processing in Phase II if their centroids lie "sufficiently" close to the coarse position of the target supplied by the tracking system. The pre-processing of plots provided in this phase is not essential to the operation of the core algorithm in Phase II but it significantly improves its computational efficiency.

In Phase II, the distances between each plot centroid in one scan and each plot centroid in the following scan are enumerated. Plots are then "paired" if their distances lie within a specified interval, and are considered to be "feasible" segments of the trajectory of the specified target. The bounds of the selection interval are derived from the coarse estimates of the target speed supplied by the tracking system. A simple heuristic strategy is utilised to further reduce the number of feasible trajectory segments and the segments are synthesised into complete trajectories, each of which corresponds to an uninterrupted sequence of target detections. It should be noted that although the algorithm is intended to obtain the trajectory of the specified target, the trajectories of nearby targets, if present, will also be obtained. However, this was only found to occur when targets were flying in formation or when flight paths intersected. In this situation the targets were located too

close together to be removed by Phase I. Finally, the extraction time corresponding to each plot centroid which comprises a trajectory is determined.

3. DESCRIPTION OF THE ALGORITHM

In order to concisely describe the processes underlying the operation of the algorithm, a mathematical treatment is provided in preference to a computer program listing or a flowchart. Set-theoretic notation was selected as the most appropriate because the processes involve the manipulation of objects, namely plots and tracks. The mathematical notation is summarized on page 17.

3.1 Data description

The historical motion of all of the targets traversing the detection volume of a surveillance radar over a finite interval of time Δt_0 can be represented by an ordered set Ψ containing the position and velocity estimates recorded from a tracking system track file. Dependent upon the method used to record the data, the set may, or may not, contain a complete history of track updates.

Due to the presence of false alarms and reinitialised tracks, the number of tracks, N, recorded generally exceeds the number of different targets present during the tracking interval Δt_0. Reinitialisation involves the assignment of a new track to a target whose previous track was deleted as a result of the target being undetected by the sensor for several scans; the incorrect placement of the track manoeuvre gate; or the selection of the wrong plot when several plots lie within the manoeuvre gate.

An individual track history is a member of the partition Ψ_0 of Ψ, viz,

$$\psi_\alpha \in \Psi_0 \text{ for all } \alpha = 1,2,\ldots,N$$

whose elements can be represented as ordered triples

$$\langle \underline{R}_i^\alpha, \underline{V}_i^\alpha, T_i^\alpha \rangle \in \psi_\alpha \text{ for all } i = 1,2,..,L_\alpha$$

where $\underline{R}_i^\alpha$ and $\underline{V}_i^\alpha$ are the tracking system estimates of the position vector $\underline{r}$ and instantaneous velocity vector $\partial \underline{r}/\partial t$ respectively of the target associated with the i-th update of track α at time $t = T_i^\alpha \in \Delta t_0$. The indexed track update times are chronologically ordered such that $T_1^\alpha < T_2^\alpha < \ldots < T_{L_\alpha}^\alpha$.

A north-mark event occurs each time the radar antenna is aligned to magnetic north and is accompanied by the extraction of an RTQC plot. The sequence of RTQC plots is assumed to be uninterrupted over the tracking interval. If interruption does occur, the algorithm will not operate correctly on a complete track; however, a block of sequential updates (viz a segment) of the track can be processed provided an uninterrupted sequence of RTQC plots occurred during the interval between the first and last updates of the segment. A track may therefore be processed in a piece-meal fashion by two (or more) applications of the algorithm. Another

assumption is that there is negligible delay between the occurrence of a north-mark event and the recording of an RTQC plot. The set of RTQC plot recording times, Λ, therefore corresponds to the set of north-mark times.

There is also assumed to be negligible delay between the extraction and recording of plots. Each plot contains an estimate of the range and azimuth of the centroid of a potential target. The set P is defined to comprise the ordered pairs $\langle \underline{r}, t \rangle$ of plot centroids (viz position vectors $\underline{r}$) and the corresponding plot extraction times (t).

The north-mark and plot centroid data to be analysed are restricted to the time interval $\Delta t_\alpha = [T_0^\alpha, T_{L_\alpha}^\alpha] \subseteq \Delta t_0$. The time T_0^α is an estimate of the time of extraction of the plot that initiated track α. Note that it is not the actual time of extraction of the plot, but only a conservative estimate of the earliest time of extraction. The symbol must also not be confused with a track update time; it is strictly the lower limit of the time interval which determines the elligibility of plots for processing by the algorithm. The upper limit of this interval is the time of the last track update.

Let $\Lambda^\alpha = \Lambda \bigcap \Delta t_\alpha$ be the set of north-mark times over the duration of track history α and define the disjoint subsets $\Lambda_i^\alpha \subset \Lambda^\alpha$ whose elements are the north-mark times prior to the track update time T_i^α (where $i = 1,2,..,L_\alpha$), viz,

$$\Lambda_i^\alpha = \{t^0 \in \Lambda^\alpha : t^0 < T_i^\alpha\}$$

A scan is precisely defined as an interval of time between consecutive north-mark events. The antenna rotation period, and hence the duration of a scan, is assumed to be a constant, T_s.

The time at the start of the j-th scan prior to the i-th track update is then given by

$$t_{i1}^0 = \text{Max}(\Lambda_i^\alpha)$$

and

$$t_{ij}^0 = \text{Max}(\Lambda_i^\alpha - \bigcup_{n=1}^{j-1} \{t_{in}^0\}) \text{ for all } j=2,3,\ldots,J_i,$$

where $J_1 = \#(\Lambda_i^\alpha)$ and $J_i = \#(\Lambda_i^\alpha - \Lambda_{i-1}^\alpha)$ for $i \neq 1$.

The notation Max(•) denotes the largest element of a finite set (ie a set with a countable number of elements) whilst #(•) denotes the number of elements in a set (ie cardinality). The north-mark timing diagram is depicted in figure 2 (p 21).

Since P is the set of target position measurements obtained from the plots over the interval Δt_0, the subset $P_0 \subseteq P$ of measurements over the duration of track history α is given by

$$P_0 = \{<\underline{r},t> \varepsilon P : t \varepsilon \Delta t_\alpha\}.$$

3.2 Phase I processing

3.2.1 Selection of plots

Since interest lies only in those plots that are likely to have been associated with the track history α, spatial filtering is employed to eliminate plots that were not located within the vicinity of the track.

If the internal processing delays in the DTE and the tracking system are minimal, the position (and time of detection) of a target can be estimated from the centroid closest to the track coordinate (and corresponding recording time) of the plot extracted prior to the track update. The delays in the DTE and tracking system vary according to their respective processing loads but the average delays are assumed to be negligible compared with the average delay in the recording of the track data.

The track data available for analysis were obtained by periodically recording the entire contents of the Myriad track file. Since the updating of the Myriad track file occurs immediately after each plot is received from the DTE, each record of track data captures only an instantaneous "snapshot" of the state of the tracks in Myriad. The intervals between these snapshots were approximately constant and asynchronously timed with respect to north-mark events. The track update times are assumed to correspond to the snap-shot recording times. The delay between any track update and its subsequent recording therefore varies, but it is always less than one scan period provided the interval between consecutive recordings is greater than one scan period. If the recording interval is greater than one, but less than two scan periods, the uncertainty in the recording delay makes it impossible to ascertain which scan contained the plot responsible for a given track update. In this case, the required plot may be found either in the scan which was either completed immediately prior to the track update, or in the ensuing scan.

Assuming that the track data recording interval exceeds two scan periods, one or more scans of plot data will be present between track updates. The position of the target in the first scan prior to the i-th track update can be estimated with reasonable accuracy from the track coordinate, $\underline{R}_i^\alpha$. The position of the target in any earlier scan (which must commence after the (i-1)-th track update) can be estimated with more accuracy from the plot data by a recursive procedure which will now be described. The procedure enables the plots which established the track (ie plots extracted immediately prior to the time of the first track update) to be selected, but it cannot process plots recorded after the last track update. This is not a limitation since any plots associated with the target after the last update are likely to have been associated with another track and may thus be processed accordingly.

Define a partition $\{P_{ij}\}$ of P_0 whose members contain only the plot data in the j-th ($j=1,2,\ldots,J_i$) scan completed prior to the i-th ($i=1,2,\ldots,L_\alpha$) track update for the target. Figure 3 (p 21) illustrates the partitioning of P_0.

The sets

$$P_{ij} = \{<\underline{r},t> \varepsilon P_0 : t \varepsilon [t^0_{i,j+1}, t^0_{ij}) \} \text{ for all } j < J_i$$

comprise the plot data in the scans that occurred between consecutive track updates, and the sets

$$P_{i,J_i} = \{<\underline{r},t> \varepsilon P_0 : t \varepsilon [t^0_{i-1,1}, t^0_{i,J_i}) \} \text{ for } i \neq 1.$$

comprise the data in those scans that included track updates. Because each of the plot centroids in a given scan are unique, the domain $Dom(P_{ij}) = \{\underline{r}: <\underline{r},t> \varepsilon P_{ij}\}$ of each set P_{ij} may be totally ordered such that every pair of elements $\underline{r},\underline{r}^* \varepsilon Dom(P_{ij})$ satisfies the relation:

$$\text{(i)} \quad \theta(\underline{r}) < \theta(\underline{r}^*)$$

or

$$\text{(ii)} \quad |\underline{r}| < |\underline{r}^*| \text{ if } \theta(\underline{r}) = \theta(\underline{r}^*),$$

where $\theta(\bullet)$ is the angular displacement of a position vector from magnetic north measured in the sense of the antenna rotation.

(Note that the range $Rng(P_{ij}) = \{t: <\underline{r},t> \varepsilon P_{ij}\}$ of each set P_{ij} can only be partially ordered because two or more plots may have identical extraction times).

In each scan the target is assumed to be located somewhere within a circular neighbourhood centred on the estimated target position obtained by the recursive procedure previously described in this section. Any plot whose centroid falls within the neighbourhood is considered likely to be the required plot and is consequently selected for Phase II processing. The radius of the neighbourhood is adjusted in each scan in proportion to the uncertainty in each target position estimate.

The sets of plot data $\hat{P}_{ij} \subseteq P_{ij}$ selected from the initial scans (j=1) are given by

$$\hat{P}_{i1} = \{<\underline{r},t> \varepsilon P_{i1} : |\underline{r} - \underline{R}^\alpha_i| < \rho_0\}.$$

The radius of the neighbourhood in the initial scans is chosen to be a fixed value ρ_0, that is sufficiently large to ensure that additional tracking errors introduced by manual tracking do not inhibit the

processing of the plots. A 10 n mile value was initially selected when testing the algorithm. Once the algorithm was validated this value was reduced by trial and error.

In order to simplify the notation, the minimum (Euclidean) distance between an arbitrary point whose position vector is $\underline{r}$ and the plot centroids contained in the set $\hat{P}_{ij}$ is defined by

$$d_{ij}(\underline{r}) = \text{Min}(\{|\underline{r}-\underline{r}^*| : \underline{r}^* \in \text{Dom}(\hat{P}_{ij})\})$$

where Min(•) denotes the smallest element in a finite set.

The target position estimate in each initial scan is given by:

$$\hat{\underline{r}}_{ij} = \begin{cases} \underline{R}_i^{\alpha}, \text{ if } \hat{P}_{i1}=\emptyset \text{ (null set), otherwise} \\ \\ \underline{r} \in \text{Dom}(\hat{P}_{i1}) : |\underline{r}-\underline{R}_i^{\alpha}|=d_{i1}(\underline{R}_i^{\alpha}). \end{cases}$$

The corresponding times of the above estimates are

$$\hat{t}_{i1} = \begin{cases} T_i^{\alpha} \text{ if } \hat{P}_{i1}=\emptyset, \text{ otherwise} \\ \\ t : <\hat{\underline{r}}_{i1},t> \in \hat{P}_{i1}. \end{cases}$$

In the other scans ($j=2,3,..,J_i$) the sets of selected plot data are given by

$$\hat{P}_{ij} = \{<\underline{r},t> \in P_{ij} : |\hat{\underline{r}}_{i,j-1}-\underline{r}| < V_{max}^{\alpha} T_s \text{ Round } [(\hat{t}_{i,j-1}-t)/T_s] \},$$

where Round(•) denotes the nearest integer approximation to a real number.

The radius of the neighbourhood is calculated to be the maximum distance that the target could have travelled in an integral number of scan periods at the maximum speed indicated from the track history, ie

$$V_{max}^{\alpha} = \underset{i \in \{1,2,\ldots,L_{\alpha}\}}{\text{Max}} |\underline{V}_i^{\alpha}| .$$

The target position estimates are

$$\hat{\underline{r}}_{ij} = \begin{cases} \hat{\underline{r}}_{i,j-1} \text{ if } \hat{P}_{ij}=\emptyset, \text{ otherwise} \\ \\ \underline{r} \in \mathrm{Dom}(\hat{P}_{ij}) : |\underline{r}-\hat{\underline{r}}_{i,j-1}|=d_{ij}(\hat{\underline{r}}_{i,j-1}) \end{cases}$$

and the corresponding times of these estimates are

$$\hat{t}_{ij} = \begin{cases} \hat{t}_{i,j-1} \text{ if } \hat{P}_{ij}=\emptyset, \text{ otherwise} \\ \\ t : <\hat{\underline{r}}_{ij},t> \varepsilon\ \hat{P}_{ij}. \end{cases}$$

3.2.2 Resequencing of selected plots

Prior to further processing, the sets containing the selected plot data must be mapped into equivalent sets indexed by scan number; a process which essentially changes the number of set subscripts from two to one.

Let k represent the chronological sequence number, or index, of the scans contained within the time interval Δt_α, so that k=1 denotes the first scan commencing at time $t=t^0_{1,J_1}$. Then, k=2 denotes the second scan starting at $t=t^0_{1,J_1-1}$ for $J_1>1$ (or $t=t^0_{2,J_2}$ if $J_1=1$), and so on up to $k=K_\alpha=(\sum_{1\le i\le L_\alpha} J_i)-1$ which denotes the last (completed) scan commencing at $t=t^0_{L_\alpha,2}$.

The set of filtered plot data in scan k ($k=1,2,\ldots,K_\alpha$) is hence given by

$$S_k = \hat{P}_{i,j-1},$$

where the index k is the value of the bijection

$$f:\bigcup_{i=1}^{L_\alpha} [\{i\}\times\{1,2,\ldots,J_i\}]\rightarrow\{1,2,\ldots K_\alpha\},$$

viz, $k=f(k,j)=1-j+\sum_{1\le m\le i} J_m$, for all $j=1,2,\ldots,J_i$ and for all $i=1,2,\ldots,L_\alpha$.

3.3 Phase II processing

3.3.1 Computation of feasible trajectory segments

Due to random errors in the processing and recording of plot and track data, the distances travelled by a target in each scan could not be accurately determined. It is assumed that the distance traversed in each scan is randomly distributed with a mean and standard deviation given by $V_\mu^\alpha T_s$ and $V_\sigma^\alpha T_s$, respectively, where V_μ^α and V_σ^α are the mean and standard deviation of the tracking system estimates of the target speed computed over the duration of the track history, viz,

$$V_\mu^\alpha = \sum_{1 \le i \le L_\alpha} |\underline{V}_i^\alpha| / L_\alpha$$

and

$$V_\sigma^\alpha = \sqrt{\left[\sum_{1 \le i \le L_\alpha} |\underline{V}_i^\alpha|^2 / L_\alpha - (V_\mu^\alpha)^2 \right]}$$

A trajectory segment is defined as an ordered pair of plot centroids $\langle \underline{r}, \underline{r}' \rangle$, obtained from two plots in consecutive scans, and represents a sequence of two coordinates that could form part of the target trajectory. A trajectory segment is termed "feasible" if the distance between the plot centroids lies within $\pm \xi V_\sigma^\alpha T_s$ of the mean distance $V_\mu^\alpha T_s$ traversed by the target over a one scan period, where $\xi < V_\mu^\alpha / V_\sigma^\alpha$ is a positive constant which is empirically determined.

The set of feasible trajectory segments between the position estimates $\underline{r} \varepsilon S'_k = \mathrm{Dom}(S_k)$ in scan k and $\underline{r}' \varepsilon S'_{k+1} = \mathrm{Dom}(S_{k+1})$ in scan (k+1) is therefore given by:

$$G_k = \{ \langle \underline{r}, \underline{r}' \rangle \varepsilon \, S'_k \times S'_{k+1}) : \; | |\underline{r} - \underline{r}'| - V_\mu^\alpha T_s | \le \xi V_\sigma^\alpha T_s \}; k = 1, 2, \ldots, K_\alpha - 1$$

An example which demonstrates the selection of feasible trajectory segments is presented in figure 4 (p 22).

3.3.2 Reduction of the number of feasible trajectory segments

The number of feasible trajectory segments can be reduced by making two general assumptions, namely that:

(1) unique target positions are extracted during each scan, and

(2) the shortest trajectory segments are the most likely to be associated with a target.

The first assumption is based upon the extremely low probability that two or more targets are located in the same DTE resolution cell during

the same scan. Consequently, a feasible trajectory segment in G_k is only considered to form part of the same trajectory as a feasible trajectory segment in G_{k+1} if it shares a common plot centroid in scan k+1. The set of common plot centroids in each scan can be defined by

$$A_k = Rng(G_k) \bigcap Dom(G_{k+1}) \text{ for } k = 1,2,\ldots,K_\alpha-1$$

In the absence of data beyond scan K_α, each plot centroid in scan K_α is considered likely to terminate a trajectory; thus,

$$A_{K_\alpha} = Rng(G_{K_\alpha-1}).$$

The second assumption permits a trajectory segment to be selected from alternative trajectory segments in G_k, on the basis of minimum plot centroid separation distance. Although it is more intuitive to select those segments which best approximate the mean target traverse distance $V_\mu^\alpha T_s$, the minimum segment length strategy proved to be easier to implement, particularly in ranking alternative segments which have equal lengths, and yielded satisfactory results with empirical data.

The strategy operates as follows and is illustrated by a worked example in figure 5 (p 23). Initially, the trajectory segments are ranked in ascending order of plot centroid separation distance; those which have equal separation distances are sub-ranked in ascending order of the angular offset of their second coordinate vector; and those which have equal separation distances and angular offsets are further sub-ranked in ascending order of the length of their second coordinate vector. Then the first-ranked segment, the one with the shortest separation distance, is selected and its plot centroids are noted. Next, the segment with the lowest ranking whose centroids do not correspond to the first is selected. Then the segment with the lowest ranking whose centroids do not correspond to the two previously selected centroids is selected. This iterative selection process continues until a total of $\#(A_k) \leq \text{Min}\{\#(S_k'),\#(S_{k+1}')\}$ trajectory segments are selected.

The process is formally described by letting

$$X_k = \{<\underline{r},\underline{r}'>\varepsilon\ G_k,\ \underline{r}'\varepsilon\ A_k\}$$

denote the (non-empty) subset of G_k whose range is identical to the set A_k. Let X_k be totally ordered such that every distinct pair of elements $<\underline{r},\underline{r}'>,<\underline{r},\underline{r}^*> \varepsilon\ X_k$ satisfies the relation:

(i) $|\underline{r}-\underline{r}'| < |\underline{r}-\underline{r}^*|$

or (ii) $\theta(\underline{r}') < \theta(\underline{r}^*)$ if $|\underline{r}-\underline{r}'| = |\underline{r}-\underline{r}^*|$

or (iii) $|\underline{r}'| < |\underline{r}^*|$ if $\theta(\underline{r}') = \theta(\underline{r}^*)$ and $|\underline{r}-\underline{r}'| = |\underline{r}-\underline{r}^*|$.

Define $X_k^{(p)}$ (for each iteration $p=1,2,\ldots,\#[A_k]$) to be subsets of

X_k such that

$$X_k^{(p)} = \{<\underline{r},\underline{r}'> \varepsilon\ X_k^{(p-1)}:\ \underline{r} \neg\varepsilon\ \mathrm{Dom}[H_k^{(p-1)}],\ \underline{r}' \neg\varepsilon\ \mathrm{Rng}[H_k^{(p-1)}]\}$$

where

$$X_k^{(1)} = X_k \text{ and } H_k^{(p)} = \{\mathrm{Min}[X_k^{(p)}]\}.$$

Note that in the above expression "Min" specifies the element in the set $X_k^{(p)}$ which satisfies the ordering relation with respect to every other element in the set.

The reduced set of feasible trajectory segments $\hat{G}_k \subseteq G_k$ is therefore given by

$$\hat{G}_k = \bigcup_p H_k^{(p)}$$

3.3.3 Synthesis of trajectories

Trajectories of finite length, each representing an unbroken sequence of target detections, can be synthesised from the individual trajectory segments in $\bigcup_k \hat{G}_k$. The process is described below with the assistance of the worked example in figure 6 (p 24).

Only those plot centroids in the domain of $\hat{G}_k$ and not in the range of $\hat{G}_{k-1}$, are considered capable of initiating a trajectory. Excluded from consideration are those centroids in the domain of $\hat{G}_k$ which are either the intermediate (viz neither the first nor last) centroids of the trajectories initiated prior to scan k, or the centroids which terminate trajectories. Initially, each centroid in the domain of $\hat{G}_1$ is considered to initiate a trajectory.

Accordingly, the sets of plot centroids that initiate trajectories in each scan $k=1,2,\ldots,K_\alpha-1$ are specified by:

$$B_1 = \mathrm{Dom}(\hat{G}_1)$$

and

$$B_k = \mathrm{Dom}(\hat{G}_{k+1}) - \mathrm{Rng}(\hat{G}_k) \text{ for } k \neq 1,$$

For each plot centroid $\underline{r}_0^{(k)}(\ell) \in B_k$, where $\ell=1,2,\ldots,L_k = \#(B_k)$, there exists a number of other plot centroids

$$\underline{r}_m^{(k)}(\ell) : \langle \underline{r}_{m-1}^{(k)}(\ell), \underline{r}_m^{(k)}(\ell) \rangle \in G_{k+m} \text{ for all } m=1,2,\ldots,M_{k\ell} \leq (K_\alpha - k),$$

which define L_k finite sequences in the domain of P, viz,

$$C_k(\ell) = \langle \underline{r}_0^{(k)}(\ell), \underline{r}_1^{(k)}(\ell), \ldots, \underline{r}_{M_{k\ell}}^{(k)}(\ell) \rangle \text{ for } \ell = 1,2,\ldots,L_k.$$

$C_k(\ell)$ thus represents the sequence of plot centroids in the ℓ-th trajectory initiated in scan k.

The plot centroids $\underline{r}_0^{(k)}(\ell), \underline{r}_1^{(k)}(\ell), \ldots, \underline{r}_{M_{k\ell}}^{(k)}(\ell)$ are obtained from the respective scans $k,(k+1),\ldots,(k+M_{k\ell})$.

Whenever any interruption occurs in the extraction of plots by the DTE, multiple sequences of plot centroids are generated by the algorithm with each sequence being initiated in chronological order (viz, in subsequent scans). When more than one sequence is produced in a scan, it is possible that either clutter or other targets are present in the near vicinity of the target. Further attempts to localise the target must rely upon the analysis of IFF, radar height or overall (viz spatial) behaviour of the plot sequences obtained.

Because $C_k(\ell)$ is a function which maps the set of integers $\{0,1,\ldots,M_{k\ell}\}$ onto the domain of $S_k \subset P$, the set of plot data which produced the ℓ-th trajectory segment commencing in the k-th scan is given by

$$E_k(\ell) = \{\langle \underline{r},t \rangle \in S_k : \underline{r} \in \text{Rng}[C_k(\ell)]\}$$

4. COMPUTER IMPLEMENTATION

The algorithm was implemented as a computer program in the Statistical Analysis System (SAS) version 5 high level general purpose language. SAS was chosen because the plot and track data had already been translated into SAS data bases and many of the analysis programs had been written in SAS. The SAS features most extensively used in the algorithm include numerical sorting, record-oriented data structures, direct addressing of data and the statistical program library.

5. DISCUSSION

5.1 Design considerations

Operational conditions and limitations in the performance of the radar system and the recording process were factors that had to be fully considered in the design of an effective, robust algorithm. The most significant aspects are discussed below.

(1) Manual track initiation was exclusively employed during the exercise. The time taken by an operator to manually establish a track depends on his ability and experience to recognise the detection of a new target and enter the relevant information into the computer system. The delay may be considerably longer than the two scan period required for automatic initiation if the target visibility is reduced by clutter or if the operator is overloaded by the amount of information to be processed. The penalty imposed by automatic initiation is a higher frequency of false alarms. Manual initiation was employed because the false alarm rate was considered to be unacceptably high. In order to obtain maximal length trajectories, the algorithm attempts to locate plots extracted several scans prior to the time of recording of the initial track coordinate.

(2) Both data from remote sensors and visually interpreted local radar video were manually entered into the tracking system at various times during the exercise. When a track position is not manually updated, the automatic system performs the function. The algorithm must allow for the fact that manual track updates are generally less accurate compared with the automatic system.

(3) During the exercise each of the plots extracted by the DTE were recorded in sequence with minimal delay. However, only approximately one fifth of the available track data were recorded. Track updates were delayed by buffering in the Myriad track file for up to one scan period and snapshots of the track file were recorded at approximately one minute intervals. In addition, the numerical precision of the time-stamp used for marking records of plot and track data was limited to one second.

(4) The numerical precision of the recorded track coordinates was limited to one nautical mile as a result of the digital truncation of the data prior to recording. However, no loss of precision accompanied the recording of plot centroids.

(5) Some loss of accuracy occurred in the positioning of track coordinates with respect to the plot centroids due to track smoothing. Track smoothing is commonly employed in tracking systems to reduce random measurement errors. Ideally, track data for the algorithm should have been tapped from the input to the tracking filter.

5.2 Assumptions

The assumptions employed in the algorithm are listed below. The values of adjustable parameters were optimised, where possible, by trial and error to improve the operation of the algorithm.

(1) Each scan period of the AN/TPS-43F radar was assumed to be constant, $T_s = 9.375$ s. The sense of the antenna rotation was clockwise when viewed from above.

(2) The delays between the occurrence of a north-mark event and the recording of a subsequent RTQC plot, or the extraction of a primary, beacon or correlated plot and its subsequent recording, were assumed to be negligible.

(3) Due to delays in the initiation of each track, several plots may be extracted prior to the recording of the first track coordinates. The algorithm therefore commences the processing of plots $(T_1^{\alpha}-T_0^{\alpha}) = 67$ s prior to the recording of a selected track history (α).

(4) The average delay in the processing of plots by the DTE was measured to be less than 0.5 s, but on some occasions, the delay varied up to the preset maximum value of 5 s. The operation of the algorithm was only affected when the processing of plots was sufficiently prolonged to cause their extraction in a subsequent scan. Under these circumstances, the algorithm treats the delayed plots as though they are false.

(5) The maximum delay in the recording of a track update was assumed to be one scan period.

(6) The plot centroid measured in the scan which completed immediately prior to the extraction of a track coordinate was assumed to be located within a circular region of radius ρ_0 centred on the track coordinate. The radius had to be chosen large enough to allow for the additional tracking errors introduced by the manual tracking of targets. A value of 5 n mile was chosen by trial and error using a large number of track histories because it was not known which targets were manually tracked. Smaller values tended to cause gaps in some trajectories, particularly in the vicinity of sharp turns. Larger values tended to increase the number of short trajectories observed further away from the track due to false alarms.

(7) Due to random errors in the processing and recording of plot and track data, the distance that a target travelled in each scan could not be accurately determined. It was postulated that the distance traversed in each scan by a target associated with track history α was randomly distributed with a mean of $V_\mu^\alpha T_s$ and standard deviation of $V_\sigma^\alpha T_s$, where V_μ^α and V_σ^α are the respective mean and standard deviation of the track speeds over the duration of the track history.

(8) A trajectory segment was considered to be "feasible" (ie associated with the track history α) if the speed estimated from the separation of the plot centroids in consecutive scans was bounded by $V_\mu^\alpha \pm \xi V_\sigma^\alpha$. Extensive testing was performed to select an appropriate value for the constraint parameter ξ which would trade off overall computational cost against performance. $\xi = 3$ was chosen, but any value between one and three appeared to be satisfactory.

(9) It was assumed that in each scan the DTE extracted a plot for every target detected and that the plot centroids were unique. This assumption breaks down when two or more targets are located within the same resolution cell of the DTE. Under these circumstances only one plot is extracted. The size of each resolution cell was approximately 1.1° in azimuth (equal to the antenna lateral beam-width) and 0.25 n mile in slant range (equivalent to three range cell widths). When the resolution problem occurs, it persists for more than one scan as the targets shift from one resolution cell to another. The persistence may be relatively short when target trajectories cross over (eg when a target changes altitude or azimuth heading), or long when targets manoeuvre in tight formation. Under these circumstances, the algorithm is constrained to process the plot data as though only one target was present.

(10) A heuristic strategy was proposed for reducing the number of feasible trajectory segments to be synthesised into complete trajectories. The feasible segments are firstly ranked in ascending

order of plot centroid separation distance (or angular offset and length of second coordinate vectors, if the separation distances are equal). The first-ranked segment is initially selected. The second and subsequent segments are then selected as follows. The n-th ($n = 2,3,\ldots,\#[A_k]$) segment is selected which has the lowest ranking and whose plot centroids do not correspond to the first, or the second,...,or the (n-1)-th selected segment. Although this strategy is suboptimal, it produced excellent results and proved simple to implement in a computer program. It was also reasonably efficient in respect of the amount of computer processing required. More complicated strategies may further enhance the performance of the algorithm but at the cost of extra computer processing time.

5.3 The effect of noise and interrupted plot sequences

Under ideal conditions, where there are no false plots in the vicinity of the selected target and a plot is extracted for the target in every scan over the duration of its track history, the algorithm produces a continuous trajectory. Rarely were these conditions actually observed during the exercise. Several trajectories were sometimes produced because targets sporadically escaped detection by the radar and because of clutter.

In regions of intense clutter some of the false plots not removed by spatial filtering in Phase I were sufficiently correlated from scan to scan to produce feasible trajectory segments. The lengths of the resultant trajectories were generally short compared with the target trajectories due to the fact that false plot correlation distances were short. It was found that most false plots could be removed from the exercise data by rejecting the shortest trajectories (viz those comprising two plot centroids). This strategy appeared to be more effective at short range where target trajectories were longer due to more reliable detection.

Plot sequences were interrupted whenever plots associated with the target were not extracted by the DTE due to signal loss. Under these conditions, the algorithm continued to function properly, albeit producing multiple trajectories, provided the tracking system did not lose lock on the target.

It is essential to the proper operation of the algorithm that the sequence of RTQC plots is not interrupted over the tracking interval. RTQC plot extraction is substantially independent of target detection processes when the DTE is not overloaded by false plots. Delays were occasionally observed in the extraction of RTQC plots under exercise conditions but were small enough to be ignored. The only breaks in the RTQC plot sequence observed during the exercise occurred when the radar itself malfunctioned, simultaneously causing the loss of capability for tracking and the suppression of all plot data.

5.4 Description of results

Figure 7 (pp 25 to 30) depicts a representative sample of the plot centroids obtained by the algorithm from the exercise data. Each plot history corresponds to a single aircraft that was consistently tracked over a period of no less than 25 scans (4 min). The track points employed in the derivation of the plot centroids are shown in the diagrams to facilitate their comparison. Note that the vertical axes of the diagrams are aligned to magnetic north and the track coordinates were recorded at approximately one minute intervals. The consistent and accurate estimation of the target locations determined by the algorithm contrast strongly against the corresponding track coordinates.

The sample histories indicate reliable tracking of single targets with tracking errors generally accentuated in the vicinity of aircraft turns. History S125 is an exception because manual tracking appears to have been employed.

An example of the inability of the tracking system to resolve nearby targets and avoid track seduction is illustrated by history S119 in figure 8 (p 31). The trajectories produced by the algorithm indicate that three targets were present. Initially a track was established for a pair of fighter aircraft flying in close formation. The intersecting flight path of another aircraft later seduced the track. Although the paths of the fighters were almost identical and crossed in several places, it was possible for the algorithm to resolve the two aircraft because they were flying nose-to-tail (viz their flight paths were slightly staggered in time).

6. CONCLUSION

An algorithm which enables the sequences of plots associated with a selected target to be obtained from historical records of radar plot data has been described. The method involves matching plot centroids to the approximate target coordinates derived from a tracking system. The algorithm provides accurate trajectories (viz chronological sequences of plot centroids) and the set of centroid, extraction time pairs which uniquely identify the plots associated with the target.

The algorithm evolved from a requirement which arose during the analysis of the Digital Target Extractor of the RAAF AN/TPS-43F(V)-1 radar system located at 2CRU, Darwin. Because the operational data recorded during exercise Pitch Black 84-1 sometimes contained a large number of false plots, a reliable method of discriminating target-associated plots from false plots generated by system noise and clutter was required.

The coarse target position and speed estimates required by the algorithm were obtained by periodically sampling the contents of the track file of the Myriad tracking system. Plot data for the Myriad system were supplied by the DTE and provided the opportunity to extend the analysis to measuring the distribution of Myriad tracking errors. The fact that the approximate target trajectory data were derived from the same plots processed by the algorithm was coincidental. Another (viz independent) source of approximate target trajectory data, had it been available, would have been acceptable.

A set-theoretic mathematical description of the algorithm has been provided for conciseness. The assumptions employed have been empirically validated by the results obtained from its application (in the form of a SAS computer program) on the exercise data. Further development of alternative strategies in Phase II of the algorithm may further improve its performance, but at the expense of additional computer processing time.

Operational, system and recording process limitations and assumptions which affected the design of the algorithm have been described.

The effectiveness of the algorithm in discriminating target-associated plots from false plots generated by clutter or system noise has been demonstrated. A representative sample of computed target trajectories has been presented to illustrate the operation of the algorithm upon the exercise data.

The techniques employed in the algorithm appear to offer potential for the a-posteriori refinement of tracks in operational tracking systems.

7. MATHEMATICAL NOTATION

{•,•,...,•}	
or	
{•:•,...,•}	set or partition
<•,•,...,•>	sequence
<•,•>	ordered pair
<•,•,•>	ordered triple
[•,•]	closed interval
[•,•)	half open interval
Σ	summation
∂	derivative
$\subseteq$	'subset of'
$\subset$	'proper subset of'
$<$	'less than'
$\leq$	'less than or equal'
$=$	'equal'
$\neq$	'not equal'
$\equiv$	'equivalent'
$\simeq$	'approximately equal'
ε	'belongs to' (a set or class)
$\neg\varepsilon$	'does not belong to'
:	'such that'
$\rightarrow$	'mapping' (of sets)
$\cup$	set union
$\cap$	set intersection
$\times$	set product
$\|\bullet\|$	length of a vector
$\theta(\bullet)$	angular displacement of a vector
Round(•)	nearest integer approximation to a real number
Dom(•)	domain of a binary relation
Rng(•)	range of a binary relation

Min(•)	smallest element of a finite set
Max(•)	largest element of a finite set
#(•)	number of elements in a set (cardinality)
∅	null set

REFERENCES

No.	Author	Title
1	Scholz, M.L.	"Target Processing in the AN/TPS-43F-V(1) Radar Digital Target Extractor". WSRL-0570-TR, Confidential

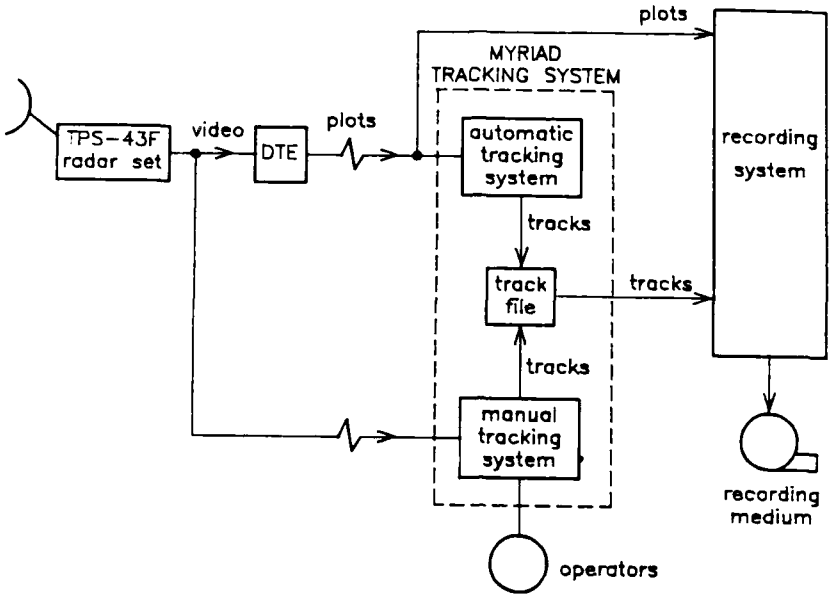

Figure 1. General data flow diagram

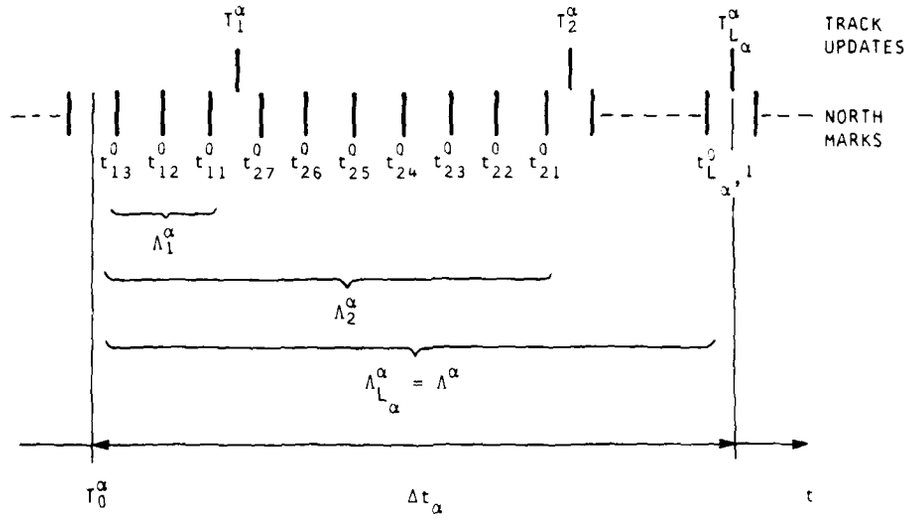

Figure 2. North-mark timing diagram

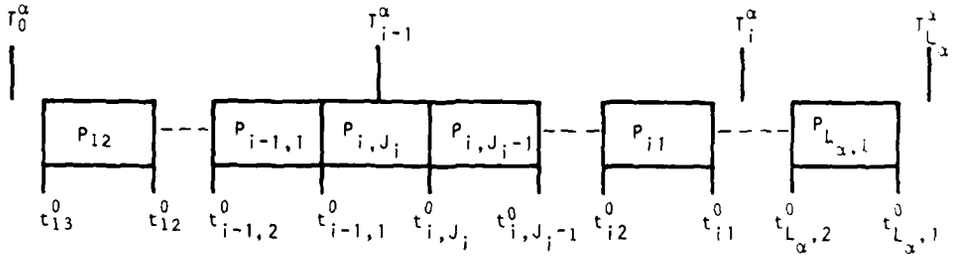

Figure 3. The partitioning of the set P_0

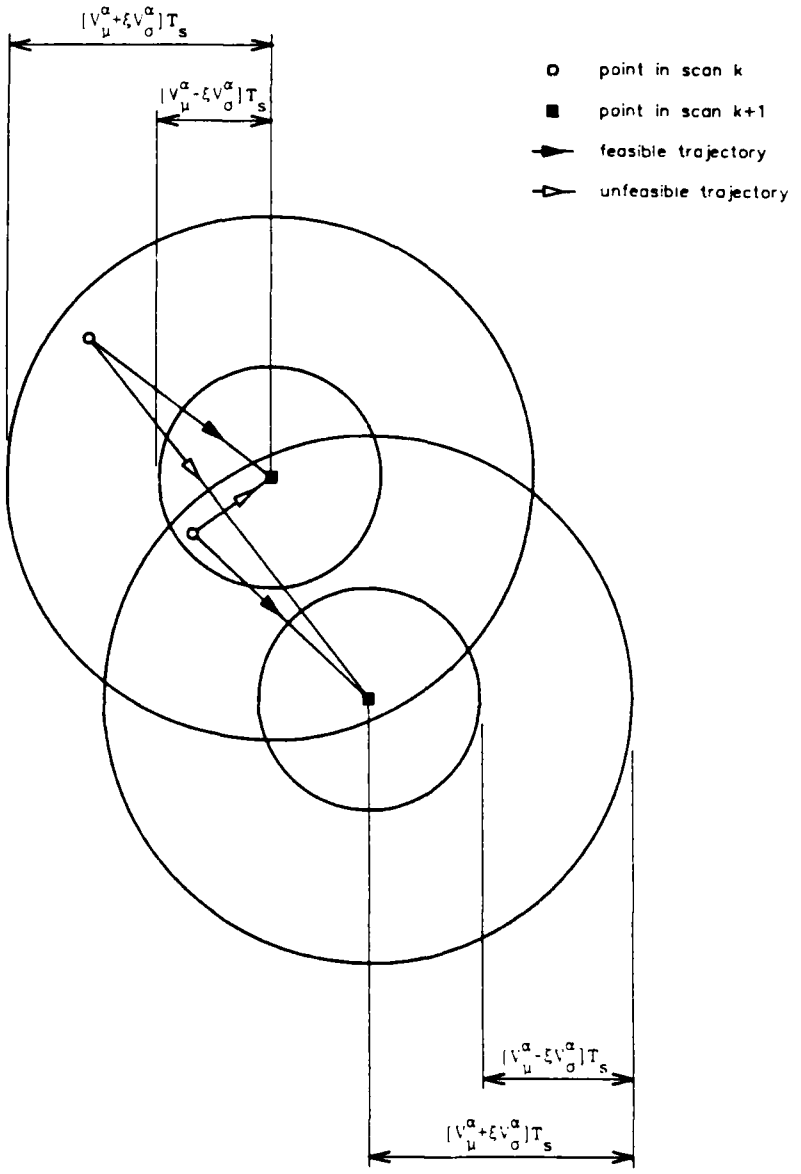

Figure 4. The selection of feasible trajectory segments

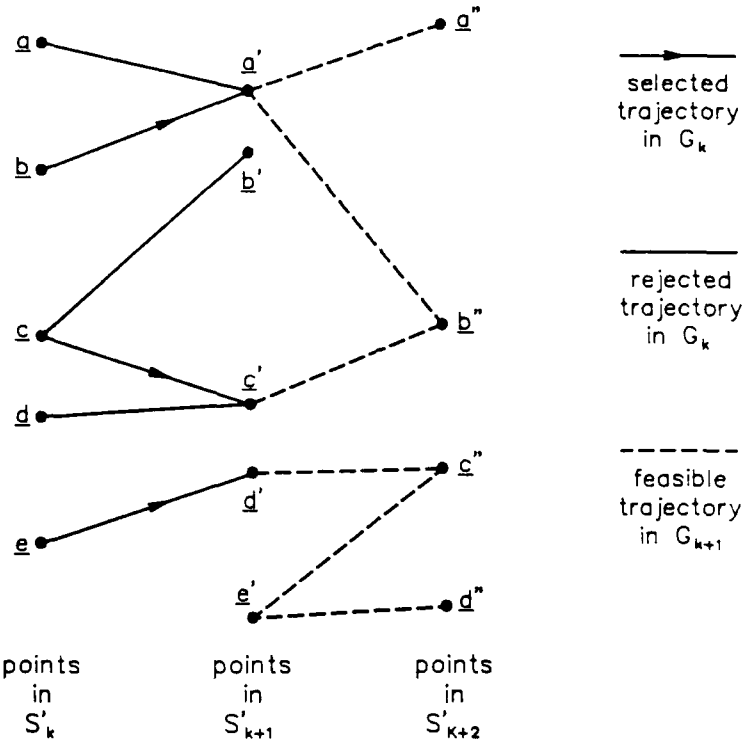

This example assumes: (1) $1<k\leq K_\alpha-2$ and

(2) G_k $=\{<\underline{a}\ \underline{a}'>,<\underline{b},\underline{a}'>,<\underline{c},\underline{b}'>,<\underline{c},\underline{c}'>,<\underline{d},\underline{c}'>,<\underline{e},\underline{d}'>\}$

(3) $G_{k+1}=\{<\underline{a}',\underline{a}">,<\underline{a}',\underline{b}">,<\underline{c}',\underline{b}">,<\underline{d}',\underline{c}">,<\underline{e}',\underline{c}">,<\underline{e}',\underline{d}">\}$

(4) $\theta(\underline{b}) < \theta(\underline{a})$

Thus, $Rng(G_k)=\{\underline{a}',\underline{b}',\underline{c}',\underline{d}'\}$, $Dom(G_{k+1})=\{\underline{a}',\underline{c}'.\underline{d}',\underline{e}'\}$,
$A_k=\{\underline{a}',\underline{c}',\underline{d}'\}$ and $\#(A_k)=3$.

Therefore, $X_k^{(1)}=X_k=\{<\underline{a},\underline{a}'>,<\underline{b},\underline{a}'>,<\underline{c},\underline{c}'>,<\underline{d},\underline{c}'>,<\underline{e},\underline{d}'>\}$ and $H_k^{(1)}=\{<\underline{c},\underline{c}'>\}$,
$X_k^{(2)}=\{<\underline{a},\underline{a}'>,<\underline{b},\underline{a}'>,<\underline{e},\underline{d}'>\}$ and $H_k^{(2)}=\{<\underline{b},\underline{a}'>\}$,
and $X_k^{(3)}=H_k^{(3)}=\{<\underline{e},\underline{d}'>\}$.

Hence $G_k=H_k^{(1)}\cup H_k^{(2)}\cup H_k^{(3)}=\{<\underline{b},\underline{a}'>,<\underline{c},\underline{c}'>,<\underline{e},\underline{d}'>\}$

Figure 5. Reduction of the set of feasible trajectory segments

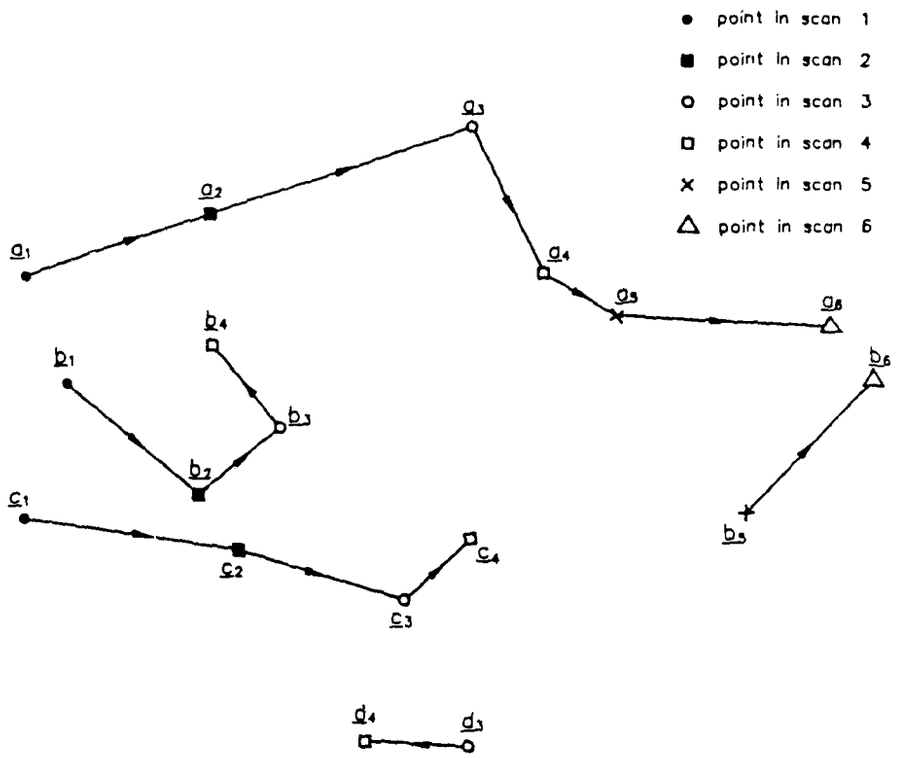

This example assumes: (1) $K_\alpha=6$ and

(2) $\underline{a}_1,\underline{b}_1,\underline{c}_1 \in S'_1$ (4) $\underline{a}_3,\underline{b}_3,\underline{c}_3,\underline{d}_3 \in S'_3$ (6) $\underline{a}_5,\underline{b}_5 \in S'_5$

(3) $\underline{a}_2,\underline{b}_2,\underline{c}_2 \in S'_2$ (5) $\underline{a}_4,\underline{b}_4,\underline{c}_4,\underline{d}_4 \in S'_4$ (7) $\underline{a}_6,\underline{b}_6 \in S'_6$

Then, $B_1=\{\underline{a}_1,\underline{b}_1,\underline{c}_1\}$, $B_2=\emptyset$, $B_3=\{\underline{d}_3\}$, $B_4=\emptyset$ and $B_5=\{\underline{b}_5\}$.
Setting $\underline{r}_0^{(1)}(1)=\underline{a}_1$, $\underline{r}_0^{(1)}(2)=\underline{b}_1$, $\underline{r}_0^{(1)}(3)=\underline{c}_1$, $\underline{r}_0^{(3)}(1)=\underline{d}_3$, and $\underline{r}_0^{(5)}(1)=\underline{b}_5$,
the trajectories are therefore given by:

$C_1(1)=<\underline{a}_1,\underline{a}_2,\underline{a}_3,\underline{a}_4,\underline{a}_5,\underline{a}_6>$, $C_1(2)=<\underline{b}_1,\underline{b}_2,\underline{b}_3,\underline{b}_4>$, $C_1(3)=<\underline{c}_1,\underline{c}_2,\underline{c}_3,\underline{c}_4>$,
$C_3(1)=<\underline{d}_3,\underline{d}_4>$, and $C_5(1)=<\underline{b}_5,\underline{b}_6>$

Figure 6. Synthesis of trajectories

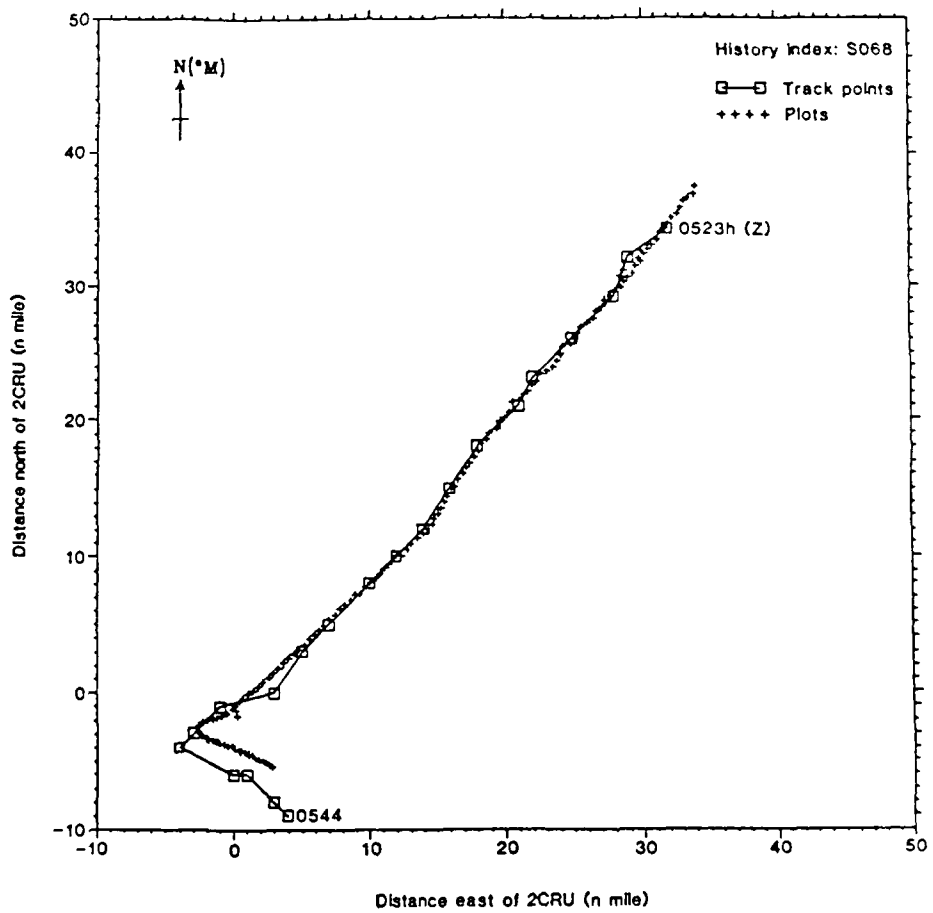

Figure 7. Typical plot-track histories of single targets

Figure 7(Contd.).

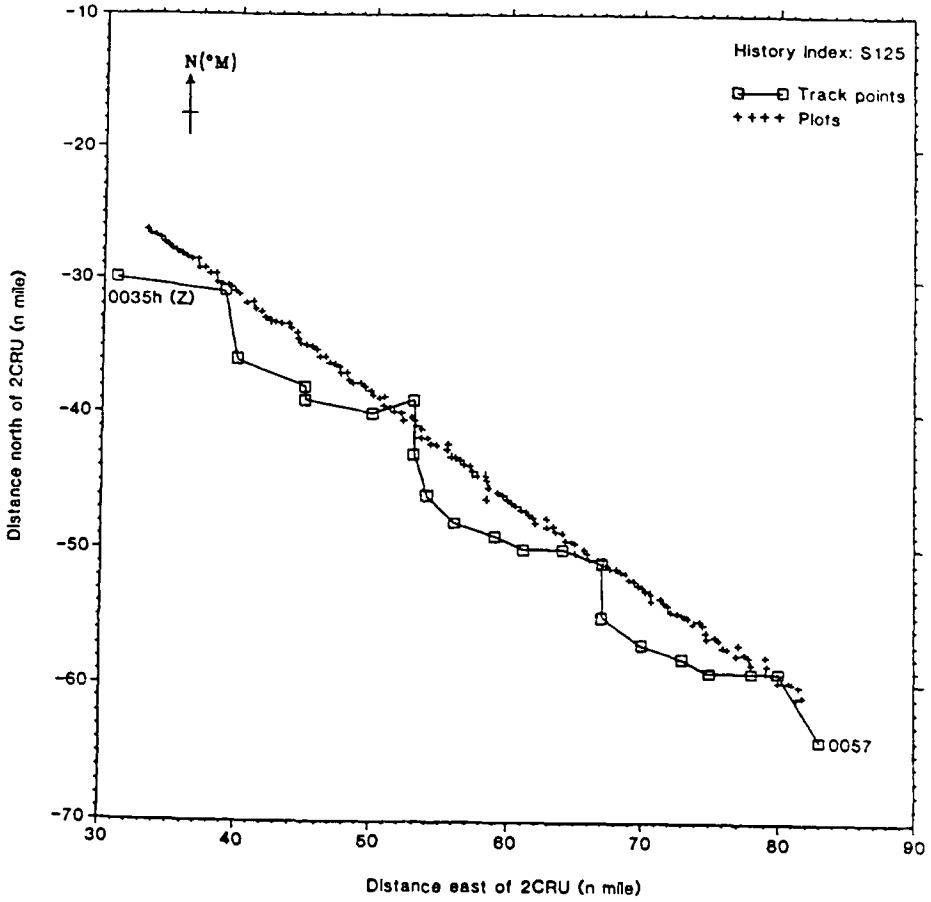

Figure 7(Contd.).

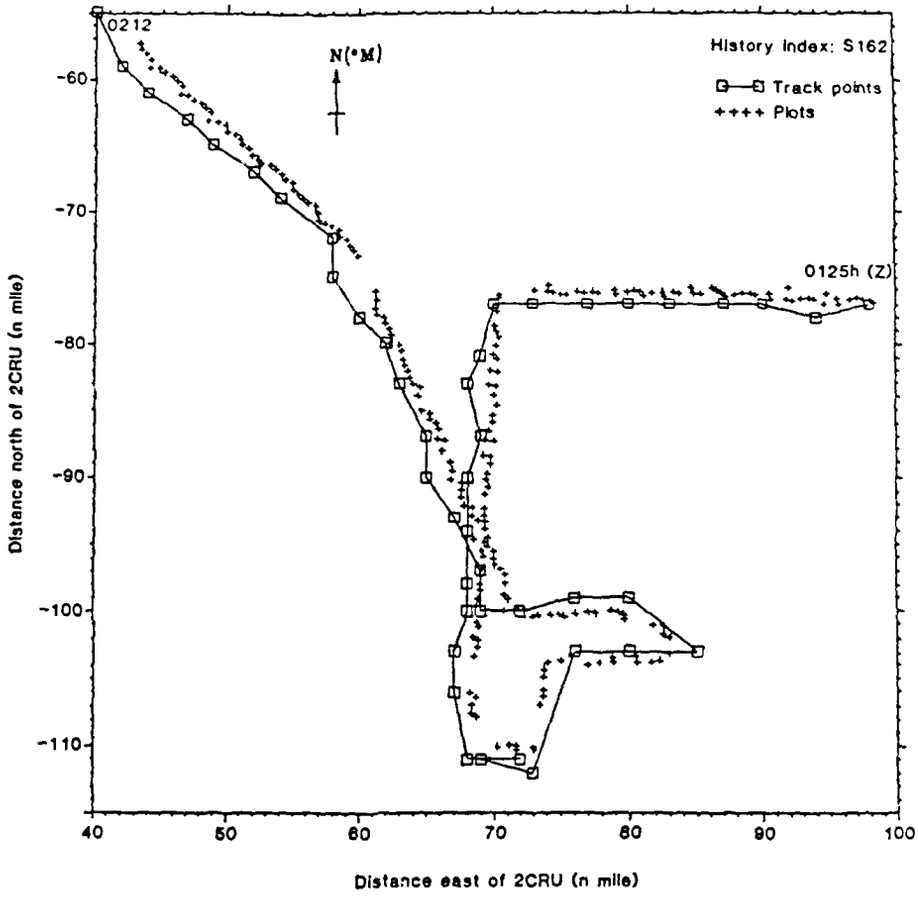

Figure 7(Contd.).

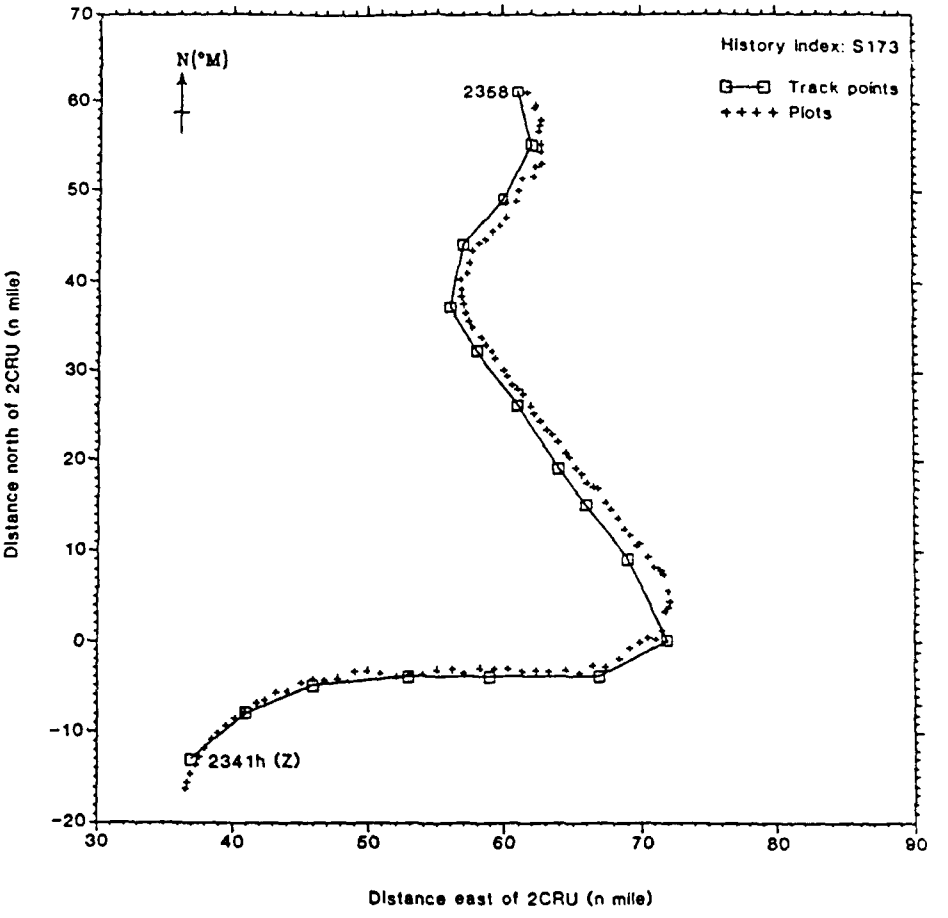

Figure 7(Contd.).

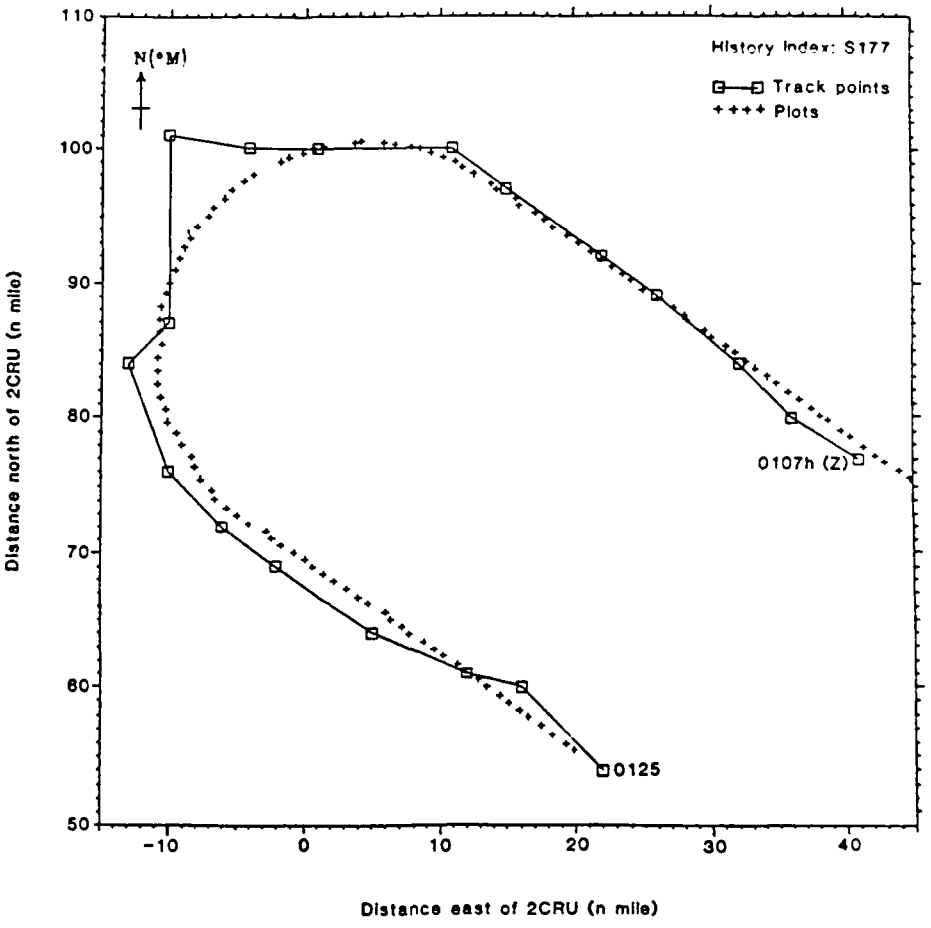

Figure 7(Contd.).

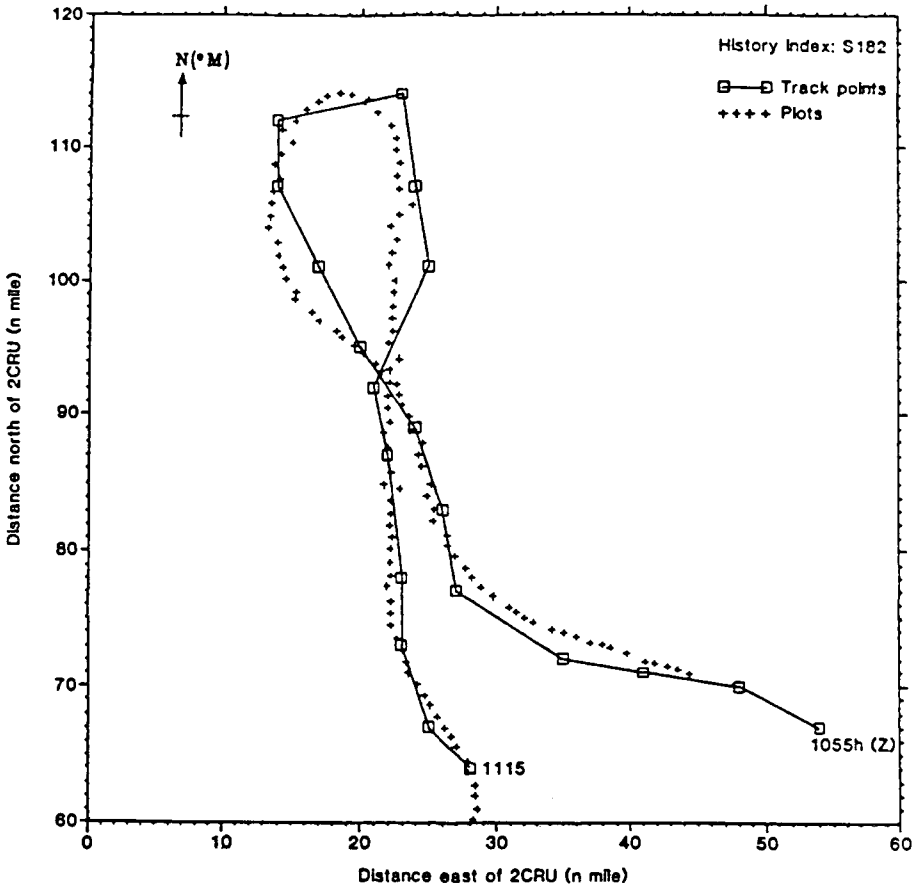

Figure 7(Contd.).

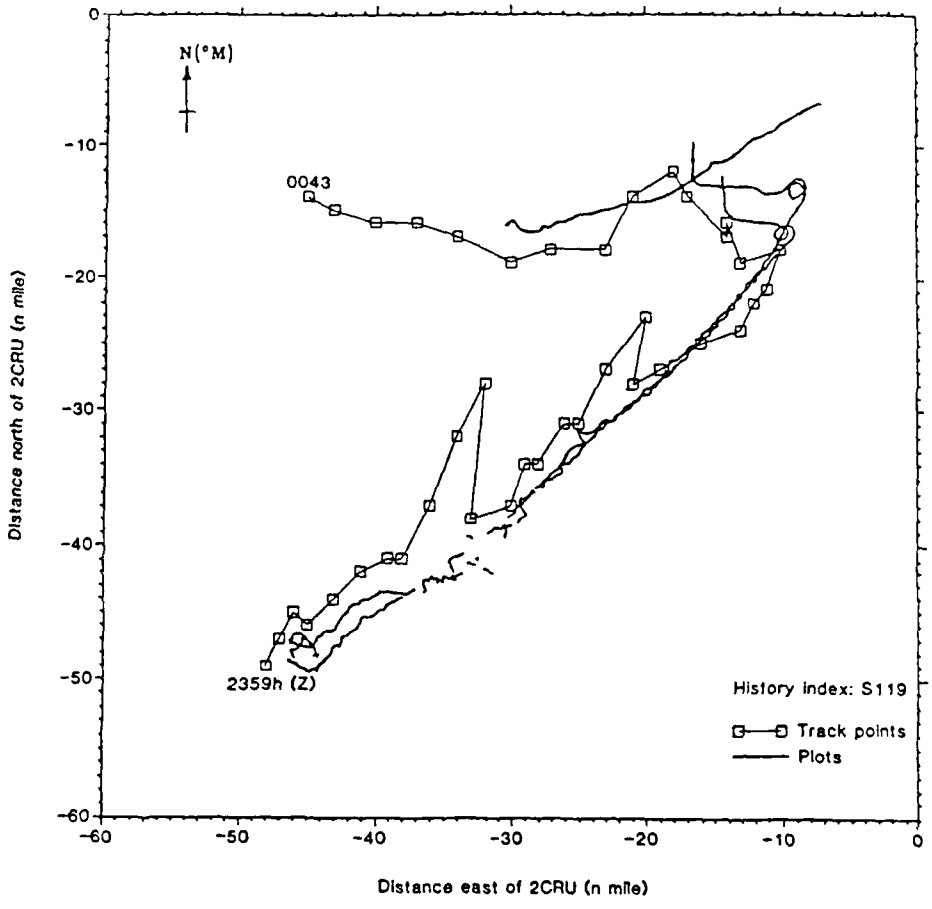

Figure 8. A typical plot-track history of multiple targets

DISTRIBUTION

	Number of copies
Defence Science and Technology Organization	
Chief Defence Scientist First Assistant Secretary, Science Policy First Assistant Secretary, Science Corporate Management Director General Science and Technology Programs	1
Counsellor Defence Science, London	Cnt Sht Only
Counsellor Defence Science, Washington	Cnt Sht Only
Weapons Systems Research Laboratory	
Director, Weapons Systems Research Laboratory	1
Chief, Combat Systems Division	1
Head, Combat Systems Integration Group	1
Head, Combat Systems Effectiveness Group	1
Head, Operations Research Group	1
M.J. Gorroick, Combat Systems Effectiveness Group	1
Dr. D.W. Keenan, Combat Systems Effectiveness Group	1
M.L. Scholz, Combat Systems Integration Group	4
Electronics Research Laboratory	
Director, Electronics Research Laboratory	1
Surveillance Research Laboratory	
Director, Surveillance Research Laboratory	1
Principal Officer, Microwave Radar Systems Group	1
Libraries and Information Services	
Librarian, Technical Reports Centre, Defence Central Library, Campbell Park	1
Document Exchange Centre Defence Information Services Branch for:	
Microfiche copying	1
United Kingdom, Defence Research Information Centre	2
United States, Defense Technical Information Center	12

Canada, Director Scientific Information Services	1
New Zealand, Ministry of Defence	1
National Library of Australia	1
Main Library, Defence Science and Technology Organization Salisbury	1
Library, Aeronautical Research Laboratories	1
Library, Materials Research Laboratories	1
Library, Aircraft Research and Development Unit	1
Library, DSD, Melbourne	1
Australian Defence Force Academy Library	1
Director of Departmental Publications	1
Department of Defence	
Joint Intelligence Organization (DSTI)	1
Air Office	
Air Force Scientific Adviser	1
Director General of Operations, Air Force	1
Director of Operational Requirements A - Air Force (Attention: ORADGE)	1
Director, Trials Directorate	1
Headquarters, Operational Command (Attention: SPLANSSO)	1
Commander Tactical Fighter Group, Williamtown	1
Officer Commanding No 41 Wing, Williamtown	1
Officer in Charge, Software Development Unit, Williamtown	1
Commanding Officer, No 2CRU, Darwin	1
Commanding Officer, No 3CRU, Williamtown	1
Commanding Officer, No 114MCRU, Amberley	1
Jindalee Project Officer, Edinburgh	1
Spares	5
Total number of copies	59

DOCUMENT CONTROL DATA SHEET

Security classification of this page : UNCLASSIFIED

1 DOCUMENT NUMBERS

AR Number : AR-005-395

Series Number : WSRL-TN-11/88

Other Numbers :

2 SECURITY CLASSIFICATION

a. Complete Document : Unclassified

b. Title in Isolation : Unclassified

c. Summary in Isolation : Unclassified

3 DOWNGRADING / DELIMITING INSTRUCTIONS

Limitation to be reviewed in August 1991

4 TITLE

THE RECONSTRUCTION OF AIRCRAFT TARGET TRAJECTORIES FROM HISTORICAL RADAR PLOT DATA

5 PERSONAL AUTHOR (S)

M.L. Scholz

6 DOCUMENT DATE

August 1988

7 7.1 TOTAL NUMBER OF PAGES 31

7.2 NUMBER OF REFERENCES 1

8 8.1 CORPORATE AUTHOR (S)

Weapons Systems Research Laboratory

8.2 DOCUMENT SERIES and NUMBER

Technical Note 11/88

9 REFERENCE NUMBERS

a. Task : 795075

b. Sponsoring Agency : RAAF

10 COST CODE

11 IMPRINT (Publishing organisation)

Defence Science and Technology Organization

12 COMPUTER PROGRAM (S) (Title (s) and language (s))

13 RELEASE LIMITATIONS (of the document)

Approved for Public Release

Security classification of this page : UNCLASSIFIED

Security classification of this page : UNCLASSIFIED

14 ANNOUNCEMENT LIMITATIONS (of the information on these pages)

No limitation

15 DESCRIPTORS

a. EJC Thesaurus Terms

Algorithms
Trajectories
Aerial targets
Tracking (position)
Radar

b. Non - Thesaurus Terms

16 COSATI CODES

0063H

17 SUMMARY OR ABSTRACT
(if this is security classified, the announcement of this report will be similarly classified)

An algorithm which can accurately reconstruct an aircraft target trajectory from pre-recorded digital radar plots is described. Periodically recorded track data from a tracking system provide the coarse target position and speed estimates required by the algorithm.

The algorithm has been applied in the operational analysis of the RAAF AN/TPS-43F(V)-1 surveillance radar and Myriad tracking systems at the No. 2 Control and Reporting Unit (2CRU), Darwin, using data acquired during exercise Pitch Black 84-1. It has proven to be reliable and effective in localising targets in the presence of clutter and system noise. Several trajectories obtained using the algorithm are illustrated and compared with the corresponding track data.